

# Accumulation of $^{10}\text{B}$ in the Central Degenerative Areas of Human Glioma and Colon Carcinoma Spheroids after Sulfhydryl Boron Hydride Administration<sup>1</sup>

Orn-Anong Pettersson,<sup>2</sup> Jörgen Carlsson, and Erik Grusell

Division of Physical Biology, Department of Radiation Sciences, Uppsala University, Box 535, S-751 21 Uppsala, Sweden

## ABSTRACT

Sulfhydryl boron hydride (BSH) ( $^{10}\text{B}$  enriched) is presently used for boron neutron capture therapy of malignant gliomas. BSH must be close to the target cells to be effective in the inactivation of cell proliferation because of the short range of the reaction products (5–9  $\mu\text{m}$ ). Clinical experience indicates that BSH is taken up in gliomas but it is not known to which structures it binds at the cellular level. *In vitro* tests on monolayer cultured cells have indicated that BSH does not bind, or only shows very weak binding, to single isolated cells. It is possible that BSH accumulates in tumor regions due to the special conditions in poorly vascularized tumor tissue, such as low  $\text{pO}_2$ , low extracellular pH, metabolic gradients, and degenerative changes. To test this we incubated three types of multicellular tumor spheroids with BSH for different times and analyzed both penetration and binding. The spatial distribution of  $^{10}\text{B}$  in sections of the spheroids was analyzed by neutron capture autoradiography. We found extensive accumulation of  $^{10}\text{B}$  in the central regions of both glioma and colon carcinoma spheroids. The accumulation closely followed the pattern of the degenerative changes which were characterized by massive necrosis in the central regions of the colon carcinoma spheroids and by a continuously increasing frequency of pyknotic nuclei as a function of depth in the glioma spheroids. The accumulation of  $^{10}\text{B}$  in the prostatic carcinoma spheroids was much lower. The penetration assay, based on freeze-drying and vapor fixation, showed that BSH penetrated easily since  $^{10}\text{B}$  equilibrated within 5–15 min in the studied spheroids. Thus, the low accumulation in the prostatic carcinoma spheroids was not due to penetration difficulties. The results of the present study on cellular spheroids and the results from previous studies on transplanted tumors support the observation that BSH penetrates easily into the degenerative tumor areas and that  $^{10}\text{B}$ , for some tumor types, might accumulate in these regions as a result of the BSH administration.

## INTRODUCTION

BNCT<sup>3</sup> is based on the  $^{10}\text{B}(n,\alpha)^7\text{Li}$  nuclear reaction. The reaction has a high thermal neutron cross-section of 3840 barn. The produced lithium ions and  $\alpha$  particles are high linear energy transfer particles. Their short range in tissue (5–9  $\mu\text{m}$ ) mainly restricts the radiation damage to those cells in which boron is located at the time of neutron irradiation. A selective uptake of  $^{10}\text{B}$  in the target cells is important for successful inactivation of cell proliferation. The principles for BNCT of cancer have recently been reviewed by Fairchild *et al.* (1), Barth *et al.* (2) and Gabel (3).

BSH is a low molecular weight substance originally tested for BNCT by Soloway *et al.* (4) and  $^{10}\text{B}$  enriched BSH is presently used for BNCT of malignant gliomas (2). The clinical experience indicates that BSH is taken up in gliomas but it is not known to which structures it binds at the cellular level. *In vitro* tests on monolayer cultured cells have indicated that BSH does not bind, or only shows very weak binding, to single

isolated cells (5, 6). It is possible that BSH accumulates in glioma tumor regions due to the special conditions, such as low  $\text{pO}_2$ , low extracellular pH, metabolic gradients, and degenerative changes that might exist in the poorly vascularized tumor tissue. To test this hypothesis we incubated three types of multicellular tumor spheroids with BSH ( $^{10}\text{B}$  enriched) for different times and analyzed both binding and penetration in the spheroids. The spatial distribution of  $^{10}\text{B}$  in sections of the spheroids was analyzed with neutron capture autoradiography.

Multicellular spheroids are considered *in vitro* models of tumor microregions (7, 8) and are used to simulate therapy with cytotoxic drugs and radiation (8–10). In this study we applied colon carcinoma, glioma, and prostatic carcinoma spheroids of human origin. The colon carcinoma and different types of glioma spheroids are well characterized regarding growth and local variations in  $\text{pO}_2$  and pH (11, 12).

## MATERIALS AND METHODS

**Cell Cultures.** Three human tumor cells lines, glioma U-343M/GaCl<sub>2</sub>:6 (hereafter called U-343M/Ga), colon carcinoma HT-29, and prostatic carcinoma, DU-145 were cultured in spinner flasks as spheroids or as monolayers in 35-mm Petri dishes. They were cultured in Ham's F-10 medium with 10% fetal calf serum, 2 mM glutamine, 100 units/ml penicillin, and 100  $\mu\text{g}/\text{ml}$  streptomycin. All cultures were incubated in high moisture air, with 20%  $\text{O}_2$  and 5%  $\text{CO}_2$ , at a temperature of 37°C. The medium was changed routinely 3 times a week. Spheroids with diameters in the range of 700–900  $\mu\text{m}$  were transferred to liquid overlay dishes (multidishes with 96 agarose coated wells; Bibby cell wells, Kebo Lab., Stockholm, Sweden) which allows experiments to be made with individual spheroids (13).

**Chemical Substance.** The BSH ( $^{10}\text{B}$  enriched) was purchased from Callery Co., Callery, PA. BSH was dissolved in distilled water and diluted with culture medium to 10 and 30  $\mu\text{g}$   $^{10}\text{B}/\text{ml}$ . The normal medium in the wells/dishes was replaced with BSH containing medium and the cultures were incubated at various time intervals. The controls were incubated in normal medium.

**Binding Studies.** The monolayers were incubated with 10  $\mu\text{g}$   $^{10}\text{B}/\text{ml}$  for 24 h and washed 2 times with complete medium and 4 times with 4°C serum free medium. The cells were treated with 0.7 ml 0.2 M acetic acid (pH 2.5) containing 0.5 M NaCl for 6 min at 4°C and then washed twice with 0.4 ml of the same solution. The remaining cells were removed by incubated with 1 N NaOH for 1 h (14). Of each solution 0.2  $\mu\text{l}$  was dropped directly on the detector and air dried (15). The control dishes were treated the same way but incubated with normal complete medium instead of boron containing medium. The spheroids were incubated with 30  $\mu\text{g}$   $^{10}\text{B}/\text{ml}$  for various times, washed twice in medium after incubation, and fixed for 1 h in neutral buffered formalin. They were thereafter dehydrated in increasing concentrations of alcohol and embedded in glycol methacrylate (Historesin; LKB-Pharmacia, Stockholm, Sweden) as has been described previously (16). Sections with a thickness of 3  $\mu\text{m}$  were cut with a glass knife in a conventional microtome.

**Penetration Study.** The spheroids were incubated in the BSH medium for 5, 15, and 30 min. Each spheroid was transferred from the BSH medium to a serum free medium drop on a plastic plate (Thermanox tissue culture cover slips, No. 5413; diameter, 13 mm; Kebo). The serum free medium was quickly absorbed by filter paper and the plate was dipped in liquid propane (cooled by liquid nitrogen) for 10 s and

Received 9/9/91; accepted 1/7/92.

The costs of publication of this article were defrayed in part by the payment of page charges. This article must therefore be hereby marked *advertisement* in accordance with 18 U.S.C. Section 1734 solely to indicate this fact.

<sup>1</sup> The work was financially supported by three grants from the Swedish Cancer Society: 980-B90-02 XB; 3009-B91-01 XAB; and 1176-B91-05 XAB.

<sup>2</sup> To whom requests for reprints should be addressed.

<sup>3</sup> The abbreviations used are: BNCT, boron neutron capture therapy; BSH, sulfhydryl boron hydride ( $\text{Na}_2\text{B}_{12}\text{H}_{11}\text{SH}$ ).

then quickly transferred to a freeze-drying instrument (Tis-U-Dry; FTS System, Inc., Stone Ridge, NY). The frozen spheroids were freeze dried overnight and thereafter fixed in formalin vapor at 80°C for 1 h. They were thereafter infiltrated with xylene, embedded in paraffin, and sectioned (5  $\mu\text{m}$ ) with a steel knife in a conventional microtome. The sections were then stretched directly on sheets of dry glass and the paraffin was removed with xylene (17).

**Neutron Autoradiography.** In this study, 500- $\mu\text{m}$  plates of polycarbonate CR-39 (allyl diglycol carbonate plates; Pershore Mouldings Limited, Pershore, England), 32-h curing time, were used since they have good discriminative properties for distinguishing between the larger tracks from the products of neutron capture in  $^{10}\text{B}$  and the smaller proton tracks from the neutron capture in nitrogen. Details of the neutron capture autoradiography technique have been described previously (18, 19). To remove the existed tracks and to enhance the sensitivity, the CR-39 plates were pretreated with 70% 6 M NaOH 30% alcohol at 70°C for 45 min (20–22). The histological sections were then pressed against the CR-39 plates by vacuum packing in plastic bags (18) in order to avoid the contribution from the nitrogen in air. The samples were irradiated with a thermal neutron fluence of  $10^{12}$ – $10^{13}$  neutrons/cm<sup>2</sup> at the autoradiography position in the thermal neutron facility at the R2-0 reactor in Studsvik, Sweden (23).

**Etching and Staining.** The CR-39 plates and the histological sections were separated after the neutron irradiation. The histological sections were stained with Mayer's hematoxylin. The CR-39 plates were etched in 6.25 M NaOH at 70°C for 1.5 h (21, 24) to enlarge the damage in the plate. The exact size of each track depends on the type and energy of the penetrating particle (25). Histological sections contain hydrogen and nitrogen which have significant neutron capture cross-sections. However, the capture reaction in hydrogen produces only  $\gamma$ -radiation and therefore no tracks in the CR-39 plates. The proton tracks from capture reactions in nitrogen are small and can be discriminated from the larger lithium and  $\alpha$  particle induced tracks in the quantitative image analysis.

**Evaluation.** The morphology of the spheroids in the histological sections was compared to the spatial distribution of the large  $\alpha$  and lithium induced tracks in the corresponding CR-39 plates. The track distributions in the CR-39 plates were evaluated by an image analysis system (Microscale TM/TC; Digithurst GmbH, Ltd., Royston, England) by setting a lower limit for the area of the single tracks. Tracks smaller than the lower limit (e.g., proton induced tracks) were excluded. A 50- $\mu\text{m}$ -wide strip along the diameter of the spheroid image was divided stepwise into intervals of 50  $\mu\text{m}$  and the relative number of tracks was counted in such 50- x 50- $\mu\text{m}^2$  areas. For the images of the spheroid, the counting started at the center of each spheroid and the values moving outward in both directions were then averaged. For the images of the droplet the number of tracks were calculated for the total area in the drops. The background values in the control preparations were withdrawn.

## RESULTS

**Background Counts.** Neutron capture processes in the glass slides and in the embedding material produced a background level of tracks. The induced tracks from the plastic embedding material were few and small but could be easily seen after irradiation with a high neutron fluence. The embedding material contained glycol methacrylate (basic resin), benzoyl peroxide (activator), and a derivative of barbituric acid (hardener) for polymer formation. The hardener contained nitrogen which contributed to the number of small proton induced tracks in the CR-39 plates. These small tracks were discriminated and did not disturb the quantitative analysis. The density of the large tracks inside and outside the plastic compartment on the glass slides was measured in control experiments. No significant differences were found.

**Accumulation of  $^{10}\text{B}$ .** In the colon carcinoma HT-29 spheroids,  $^{10}\text{B}$  accumulated extensively in the central necrosis region

as can be seen in Fig. 1b, although the viable cell layers also contained  $^{10}\text{B}$ . It can be seen in Fig. 1a that a clear border existed between the viable cell layer and the central area of necrosis. In the glioma U-343MGa spheroids, the density of the  $^{10}\text{B}$  induced tracks was significantly higher in the central than in the peripheral regions. There seem to be nearly no binding of BSH in the outer viable cells of the glioma spheroids. However, the track density increased more or less continuously with depth in the glioma spheroids (Fig. 1d) in agreement with a more or less continuous increase of the number of pyknotic nuclei (Fig. 1c). No clear border was seen between the viable and pyknotic cells in these spheroids. In the prostatic carcinoma DU-145 spheroids, there was a much lower accumulation of  $^{10}\text{B}$  than in the two other types of spheroids. It was difficult to distinguish the track density in the peripheral area of the spheroid from the track density of the background outside the spheroid section. However, there was a tendency for accumulation in the central regions as can be seen in Fig. 1f. It was, in fact, possible to observe a significant increase of the track density in the central regions of the prostatic carcinoma spheroid sections when these spheroids were irradiated with a neutron fluence 5 times higher than that used for the glioma and colon carcinoma sections. The binding of BSH was 3–4 times higher for monolayer cultured colon carcinoma HT-29 cells than for monolayer cultured glioma U-343MGa cells. The level of binding to the glioma cells was only slightly above the background level.

**Quantitative Tracks Analysis.** The relative density of large tracks from neutron capture processes in  $^{10}\text{B}$  was analyzed quantitatively in the image analyzer as a function of the distance from the center of the spheroids. A comparison of the BSH accumulation in the three types of spheroids after 24-h incubations is shown in Fig. 2 and it is clearly seen that the track density was highest in the central regions of glioma and colon carcinoma spheroids. The patterns of the curves are in accordance with the track distributions seen in the photos shown in Fig. 1. Furthermore, it can be seen in Fig. 3 that the accumulation of BSH increased as a function of incubation time in the glioma spheroids. The increase mainly took place in the deeper regions of the spheroids. The number of tracks in the periphery was low and independent of the incubation time.

**Penetration.** The colon carcinoma HT-29 and the prostatic carcinoma DU-145 spheroids were chosen for studies of the penetration of BSH since they represented the highest and the lowest accumulation, respectively. The  $^{10}\text{B}$  content was equilibrated throughout the spheroids already within 5–15 min (Fig. 4). Thus, there did not seem to be any penetration barriers for BSH in these spheroids which is in agreement with nearly free diffusion for such a low molecular weight substance (26).

## DISCUSSION

There was an extensive accumulation of  $^{10}\text{B}$  in the central regions of both the glioma and the colon carcinoma spheroids. The accumulation was, for all three types of spheroids, lower in the peripheral regions containing viable cells and the  $^{10}\text{B}$  track density closely followed the pattern of the degenerative changes. There was massive necrosis in the central regions of the colon carcinoma spheroids, in accordance with previous findings (13), and the track density was high and homogeneous in this region. The glioma spheroids were characterized by a continuously increasing frequency of pyknotic nuclei as a function of depth (27, 12); the spatial distribution of tracks followed

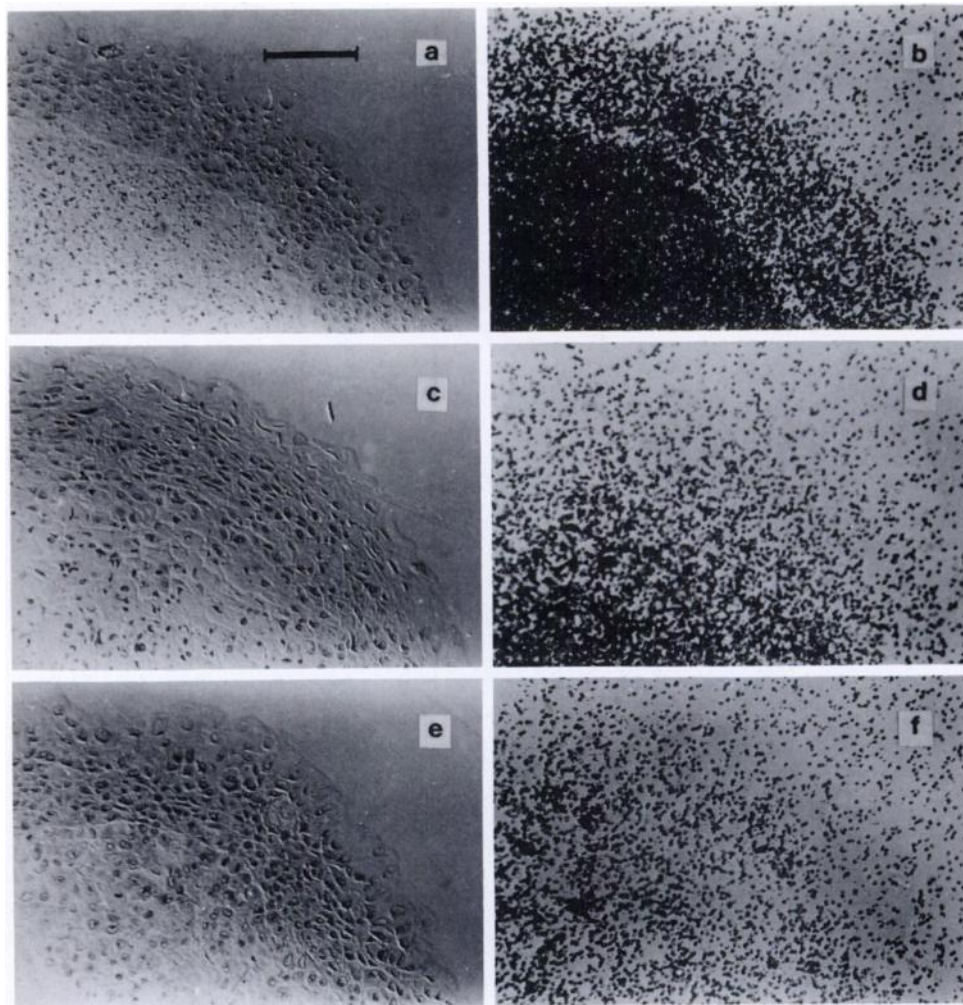


Fig. 1. Photographs of stained histological sections (left) and  $\alpha$  and lithium tracks in CR-39 detectors (right) from spheroids incubated with BSH containing medium for 24 h. Colon carcinoma HT-29 spheroids (a and b), glioma U-343MGa spheroids (c and d) and prostatic carcinoma DU-145 spheroids (e and f). The histological sections and the track detectors were irradiated with  $10^{13}$  neutrons/cm<sup>2</sup> before separation. Bar, 100  $\mu$ m.

the same pattern. Almost no <sup>10</sup>B could be detected in the outer cell layers of the glioma spheroids and in monolayer cultured glioma cells. The accumulation in the prostatic carcinoma spheroids was low and could be demonstrated only after irra-

diation with high neutron fluences. Note in Fig. 1e that the signs of pyknotic nuclei and cell degeneration in the central regions of the prostatic carcinoma spheroids were not as evident as for the colon carcinoma and glioma spheroids shown in Fig. 1, a and c.

The appearance of necrosis is a common feature in poorly

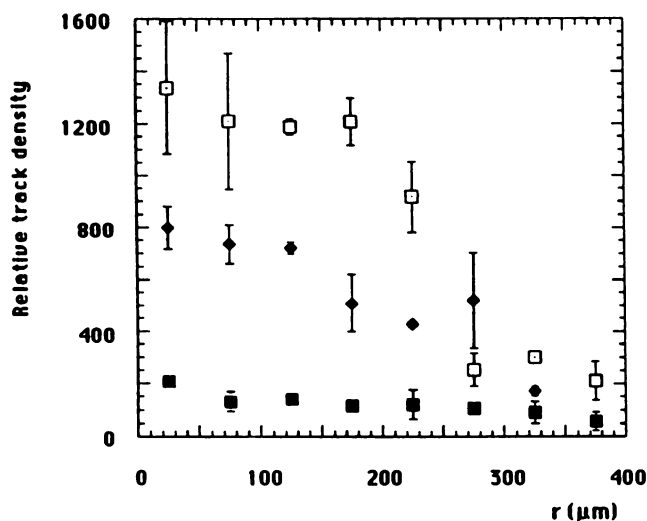


Fig. 2. Accumulation of <sup>10</sup>B, after 24 h incubation in BSH containing medium, as a function of the distance from the center, *r*, in the three different types of spheroids. The relative track densities are shown for detectors that were exposed to  $10^{13}$  neutrons/cm<sup>2</sup> together with the histological spheroid sections. □, colon carcinoma; ◆, glioma; ■, prostatic carcinoma.

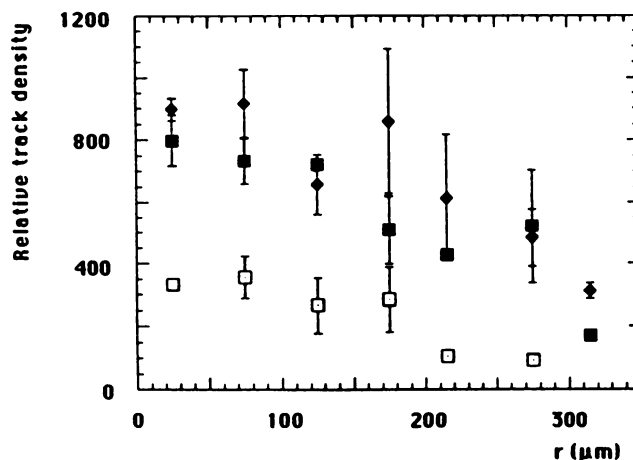


Fig. 3. Accumulation of <sup>10</sup>B after BSH administration for different times as a function of the distance from the center, *r*, in glioma spheroids. The relative track densities are shown for detectors that were exposed, together with the histological spheroid sections, to  $10^{12}$  neutrons/cm<sup>2</sup>. □, 5 h; ◆, 14 h; ■, 24 h. Bars, SD.

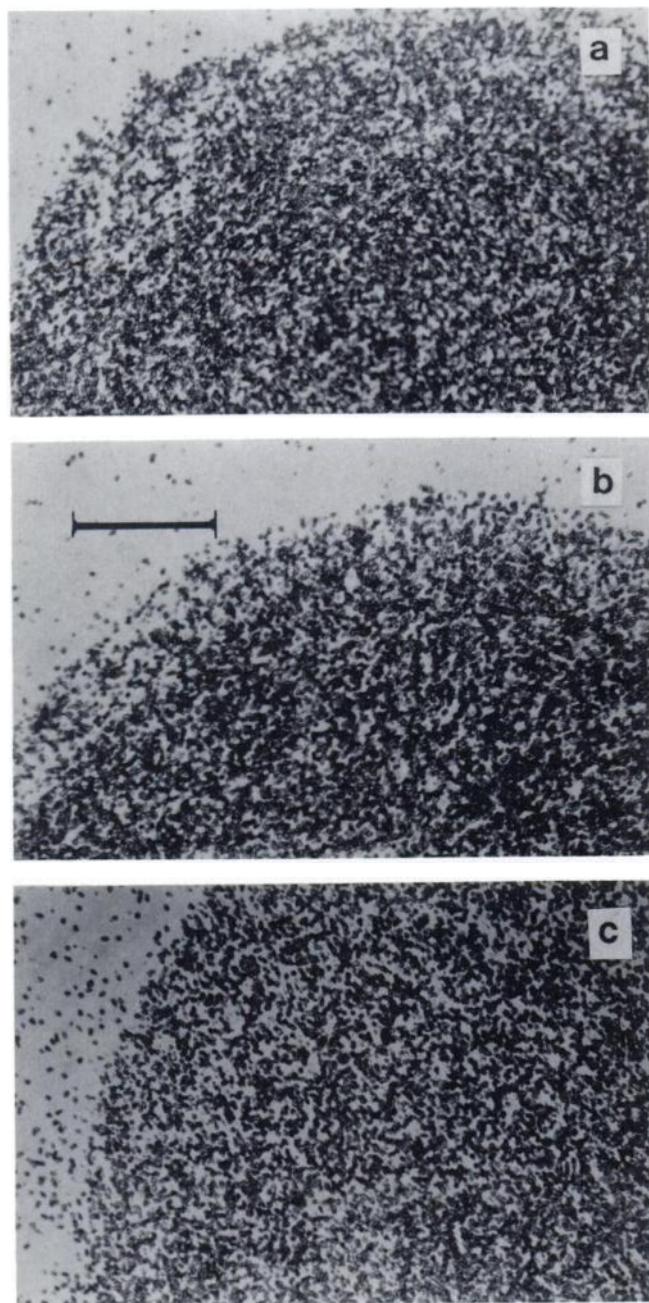


Fig. 4. Penetration of BSH in spheroids measured through the analysis of the  $^{10}\text{B}$  distribution in spheroid sections. The spheroids were frozen, freeze-dried, vapor fixed, and sectioned after BSH incubation for various times. HT-29 spheroids were incubated with BSH containing medium for 5 min. *a*, HT-29 spheroids incubated for 15 min; *b*, DU-145 spheroids incubated for 15 min; *c*, Bar, 100  $\mu\text{m}$ .

vascularized regions of tumor tissue and also in the central regions of cultured spheroids. The present hypothesis about induction of necrosis is that it is due to a combination of different stress factors of which low pH, low  $\text{pO}_2$ , and low glucose concentration might be the most important (8, 9, 11, 28). Thus, the observed differences between the gliomas and prostatic carcinomas regarding the shape of the necrotic areas are probably due to differences in the quantitative contribution of these stress factors or due to different sensitivities for the stress factors.

Thus, the  $^{10}\text{B}$  accumulation after BSH administration correlated mainly with the occurrence of degenerative changes in the studied spheroids. A possible explanation to the successful use

of BSH reported for treatments of malignant gliomas (2) might be that the substance accumulates in degenerative tumor microregions and that there might then be a slow release of BSH from these regions into surrounding viable cell layers during the neutron irradiation. Durand (10) has recently pointed out that binding of anthracyclines in some areas of a tumor and a delayed release might give an improved therapeutic effect. The situation regarding BSH can be similar.

The penetration assay, based on freeze-drying and vapor fixation, showed that BSH penetrated easily into the studied spheroids. BSH is a small molecule and should not have difficulties diffusing extracellularly into the deeper regions of the spheroids. Thus, the low accumulation of  $^{10}\text{B}$  in the prostatic carcinoma spheroids could not be explained by penetration difficulties. Furthermore, the autoradiographs in Fig. 4, showing the sum of both bound and non bound BSH, showed no gradients indicating that it was not the total concentration of BSH but only the binding that varied as a function of the depth in the spheroids.

Previous studies on transplanted tumors in mice have shown that  $^{10}\text{B}$  after BSH administration accumulated in the central regions of the tumors. Studies were carried out on implanted tumors of Harding-Passley melanoma (18) and RGC6 glioma (29) types. The  $^{10}\text{B}$  distributions were analyzed in track detector films placed on whole body sections. It was clearly seen that BSH easily penetrated and that  $^{10}\text{B}$  bound in the central and possibly degenerative areas.

Further studies should be conducted to analyze the molecular mechanisms causing the accumulation of  $^{10}\text{B}$  in the degenerative regions. The accumulation can, for example, be due to a more or less nonspecific binding of BSH to degradation products. It is also possible that BSH binds with a specific mechanism to cell debris or degenerating cells with or without pyknotic nuclei. Microenvironmental factors such as low pH and low  $\text{pO}_2$ , which are characteristic features of poorly vascularized tumor tissue, might also be of importance. Inside the spheroids at 200  $\mu\text{m}$  depth from the outer surface, the pH has been reported to decrease 0.13–0.23 and 0.25–0.46 pH units for colon carcinoma HT-29 and for different types of glioma spheroids, respectively, while the corresponding figures for the  $\text{pO}_2$  decrease was 115–135 and 70–100 mm Hg (11, 28).

The most extensive BSH binding was seen in the deeper regions of the spheroids where both the pH and the  $\text{pO}_2$  values were low. Thus, low pH or  $\text{pO}_2$ , or the combination, might be of importance for BSH binding. The HT-29 spheroids seemed to bind more BSH than the U-343MGa spheroids (Fig. 1) and since the HT-29 spheroids had lower central  $\text{pO}_2$  values the correlation between BSH binding and low  $\text{pO}_2$  seemed most obvious. However, this correlation does not, thus far, have general validity because too few cell types were studied and the observed relations might be coincident. Possible changes in the redox potential of the central regions might also influence BSH binding. BSH might be oxidized to a dimer and also react with disulfide-containing proteins. This might be processes which preferentially takes place in the central, possibly proteolytic, regions of the spheroids.

#### ACKNOWLEDGMENTS

The authors thank Lilliann Gille Grundel, Veronika Asplund, and Anki Carlsson at the division of physical biology in Uppsala for assistance with the histological preparations. The authors also thank Amilcar Roberto at the toxicology department in Uppsala for help with

the image analyzer. Per Svensson and the staff in Studsvik assisted with the neutron irradiations.

## REFERENCES

- Fairchild, R. G., Bond, V. P., and Woodhead, A. D. *Clinical Aspects of Neutron Capture Therapy*. New York: Plenum Publishing Corp., 1989.
- Barth, R. F., Soloway, A. H., and Fairchild, R. G. Boron neutron capture therapy of cancer. *Cancer Res.*, *50*: 1061-1070, 1990.
- Gabel, D. Boron neutron capture therapy for tumors: principles, problems and perspectives. *In: Publication Eurocourse: Advanced Techniques for Nuclear Medicine and Radiotherapy*. Dordrecht, The Netherlands, Kluwer Academic Publishers, 1991.
- Soloway, A. H., Hatanaka, H., and Davis, M. A. Penetration of brain and brain tumor VII. Tumor-binding sulfhydryl boron compounds. *J. Med. Chem.*, *10*: 714-717, 1967.
- Laster, B. H., Kahl, S. B., Kalef-Ezra, J., Popenoe, E. A., and Fairchild, R. G. Biological efficacy of a boronated porphyrin as measured in the cell culture. *Strahlenther. Onkol.*, *165*: 203-205, 1989.
- Fairchild, R. G., Kahl, S. B., Laster, B. H., Kalef-Ezra, J., and Popenoe, E. A. *In vitro* determination of uptake, retention, distribution, biological efficacy, and toxicity of boronated compounds for neutron capture therapy: a comparison of porphyrins with sulfhydryl boron hydrides. *Cancer Res.*, *50*: 4860-4865, 1990.
- Mueller-Kliesser, W. Multicellular spheroids. *J. Cancer Res. Clin. Oncol.*, *113*: 101-122, 1987.
- Sutherland, R. M. Cell and environment interactions in tumor microregions: the multicell spheroid model. *Science (Washington DC)*, *240*: 117-256, 1988.
- Carlsson, J., and Nederman, T. Tumour spheroid technology in cancer therapy research. *Eur. J. Clin. Oncol.*, *25*: 1127-1133, 1989.
- Durand, R. E. Slow penetration of anthracyclines into spheroids and tumors: a therapeutic advantage? *Cancer Chemother. Pharmacol.*, *26*: 198-204, 1990.
- Carlsson, J., and Acker, H. Relations between pH, oxygen partial pressure and growth in cultured cell spheroids. *Int. J. Cancer*, *42*: 715-720, 1988.
- Carlsson, J., and Acker, H. Influence of the oxygen pressure in the culture medium on the oxygenation of different types of multicellular spheroids. *Int. J. Radiat. Oncol. Biol. Phys.*, *11*: 535-546, 1985.
- Carlsson, J., and Yuhas, J. M. Liquid overlay culture of cellular spheroids. *Recent Results Cancer Res.*, *95*: 1-23, 1984.
- Haigler, H. T., Maxfield, F. R., Willingham, M. C., and Pastan, I. Dansylcadavarine inhibits internalization of  $^{125}\text{I}$ -epidermal growth factor in BALB 3T3 cells. *J. Biol. Chem.*, *255*: 1239-1241, 1979.
- Martini, F., Heurteaux, C., Wissocq, J. C., Thellier, M., and Stampfer, A. Quantitative problems in using nuclear reactions and dielectric detectors for the detection of stable isotopes ( $^6\text{Li}$  and  $^{10}\text{B}$ ) in biological samples. *J. Radioanal. Nucl. Chem.*, *91/1*: 3-16, 1985.
- Carlsson, J., Daniel-Szolgay, E., Frykholm, G., Glimelius, B., Hedin, A., and Larsson, B. Homogeneous penetration but heterogeneous binding of antibodies to carcinoembryonic antigen in human colon carcinoma HT-29 spheroids. *Cancer Immunol. Immunother.*, *30*: 269-276, 1989.
- Nederman, T., Carlsson, J., and Malmqvist, M. Penetration of radioactive labelled substances in cell spheroids. A methodological study. *In Vitro (Rockville)*, *17*: 290-298, 1981.
- Larsson, B., Gabel, D., and Börner, H. G. Boron loaded macromolecules in experimental physiology: tracing by neutron capture radiography. *Phys. Med. Biol.*, *20*: 361-370, 1984.
- Gabel, D., Hlostein, H., Larsson, B., Gille, L., Ericson, G., Sacker, D., Som, P., and Fairchild, R. G. Quantitative neutron capture radiography for studying the biodistribution of tumor-seeking boron-containing compounds. *Cancer Res.*, *47*: 5451-5454, 1987.
- Hassib, G. M., Piesch, E., and Massera, G. E. Electrochemical etching of  $\alpha$  particles in polycarbonates and applications. *In: Proceeding of the 10th International Conference on Solid State Nuclear Track Detectors*, pp. 329-335. Oxford: Pergamon Press, 1979.
- Gruhn, T. A., Li, W. K., Benton, E. V., Cassou, R. M., and Johnson, C. S. Etching mechanism and behaviour of polycarbonates in hydroxide solution: Lexan and CR-39. *In: Proceedings of the 10th International Conference on Solid State Nuclear Track Detectors*, pp. 291-302. Oxford: Pergamon Press, 1979.
- Morris, K. J., and Batchelor, A. L. The simultaneous imaging of boronated tissue sections and the location of fissionable actinide particles in CR-39 solid state track detector, utilising a neutron-induced autoradiographic technique. *Phys. Med. Biol.*, *33*: 1195-1203, 1988.
- Pettersson, O., Svensson, P., Larsson, B., and Grusell, E. Studsvik thermal neutron facility. *In: Progress in Neutron Capture Therapy for Cancer*, pp. 91-93. New York: Plenum Publishing Corp., 1992.
- Henshaw, D. L., Griffiths, N., and Landen, A. L. A method of producing thin CR-39 plastic nuclear track detectors and their application in nuclear science and technology. *Nucl. Instrum. Methods*, *180*: 65-77, 1981.
- Durrani, S. A., and Bull, R. K. *Solid State Nuclear Track Detection*. Oxford: A Wheaton & Co., Ltd., 1987.
- Nederman, T., Carlsson, J., and Kuoppa, K. Penetration of substances into tumour tissue, model studies using saccarides, thymidine and thymidine-5-triphosphate in cellular spheroids. *Cancer Chemother. Pharmacol.*, *22*: 21-25, 1988.
- Carlsson, J., Nilsson, K., Westermark, B., Pontén, J., Sundström, C., Larsson, E., Bergh, J., Pahlman, S., Busch, C., and Collins, V. P. Formation and growth of multicellular spheroids of human origin. *Int. J. Cancer*, *31*: 523-533, 1983.
- Daniel-Szolgay, E., Carlsson, J., Zierold, K., Holtermann, G., and Acker, H. Effects of amiloride treatment on U-118 MG and U-251 MG human glioma and HT-29 human colon carcinoma cells. *Cancer Res.*, *51*: 1039-1044, 1991.
- Abe, M., Amano, K., Katsutoshi, K., Tasheishi, J., and Hatanaka, H. Boron distribution analysis by  $\alpha$ -autoradiography. *J. Nucl. Med.*, *27*: 677-684, 1986.